Effects of low concentration cobalt doping on the magnetic and optical properties of $Zn_{1-X}Co_XO$ nanorods

T. KAUR[a], J. SINGH[e], B. SINGH[b,c], V. S. PANDEY[b,c], G. SINGH[a,d], M. K. NAYAK[b,c]
[a]*Shri Guru Granth Sahib World University Fathegarh Sahib, Punjab, India*
[b]*Academy of Scientific and Innovative Research, CSIR-CSIO, Chandigarh*
[c]*CSIR-Central Scientific Instrument Organization, Chandigarh 160030, India*
[d]*Lakehead University, Thunder Bay, Ontario, Canada*
eBharat Electronics Limited, Ghaziabad, India

A systematic investigation of the structural and optical properties of $Zn_{1-x}Co_xO$ (x=0.002, 0.004, 0.006 and x=0.008) nanorods synthesized by sol gel, using polyvinyl alcohol as surfactant, is presented. The formation of Co doped ZnO nanorods having size 22-28 nm, with polycrystalline behavior and wurtzite structure, is confirmed by TEM and XRD analysis. Doping concentrations of Co^{2+} ions affects the absorbance as well as magnetic properties of $Zn_{1-x}Co_xO$ nanorods. Optical absorption measurements show that for doping concentration of Co^{2+} below 1%, the bandgap has a negative correlation with the concentration. Furthermore, magnetic hysteresis curve (B-H) depicts that the behavior of $Zn_{1-x}Co_xO$ nanorods changes from ferromagnetic to antiferromagnetic by changing the Co^{2+} concentration from 0.2% to 0.8%.

(Received June 10, 2016; accepted June 7, 2017)

Keyword: Antiferromagnetic, Ferromagnetic, Nanorods, Surfactant, Wurtzite structure, Cobalt doped Zinc (ZC)

1. Introduction

III–V and II–VI semiconductors doped with transition metal-ions, exhibits both magnetic and transport properties [1,2], which leads to numerous applications in spintronic. Among these semiconductors, ZnO has gained huge interest, because of its wide bandgap (3.37 eV) and large exciton binding energy (60 meV) at room temperature. A large number of studies have reported that, cobalt doped ZnO nanostructures exhibits ferromagnetism [3-6] which depends on the percentage of Co^{2+} doping. The ionic radii of Co^{+2} (0.058nm) and Zn^{+2} (0.060nm) have similar values, thus results in greater solubility of Co^{+2} in the ZnO lattice [4]. Many research groups have investigated that, Co atomically substitutes Zn in crystal lattice leading to a substitutional solid solution. This substitution has been confirmed using a variety of characterization techniques, that include EXAFS [8,9] optical absorption [7], XPS [11,12], MCD [7, 9, 12] XAS [9,13,14], ESR [12] and XANES [13]. ZnO nanomaterial have been prepared by various methods such as metal-organic chemical-vapor-deposition [14], precipitation [18-20], spray pyrolysis [21,22], freeze drying method [19], thermal vapor deposition [20], electro deposition [21], sputtering [22], hydrothermal [27-29], pulsed laser deposition (PLD) technique [25] etc. All these synthesis methods require sophisticated equipment and are feasible at high temperature. A simple approach towards the synthesis of cobalt doped ZnO nanorods is sol-gel method, which has great potential for the production of technologically useful nanomaterials. The method has other additive features such as, time saving, low energy consumption, self-sustaining instantaneous reaction, and high yield [31-33].

This study was aimed at investigating the optical and magnetic properties of $Zn_{1-x}Co_xO$ nanorods with doping concentration of Co^{2+} below 1%. To the best of authors' knowledge, no such study involving doping concentration of Co^{2+} below 1% has been reported earlier.

2. Experimental details

$Zn_{1-x}Co_xO$ (ZC) nanorods with x=0.002, 0.004, 0.006 and x=0.008 were synthesized, via sol-gel method. The precursors used in the synthesis were polyvinyl alcohol (PVA), zinc acetate ($Zn(O_2CCH_3)_2$, 99.99%), cobalt chloride ($CoCl_2.5H_2O$, 99.99%), ethanol (C_2H_6O), acetic acid (CH_3COOH). All the analytic grade (AR) chemical reagents used in the study were procured from Sigma Aldrich.

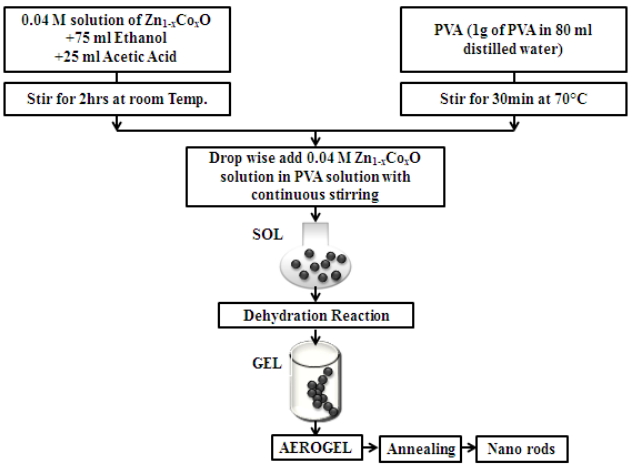

Fig. 1. Sol gel synthesis of Co-doped ZnO nanoparticles

For the preparation of 0.04 M solution of $Zn_{1-x}Co_xO$, cobalt chloride (x gram) and zinc acetate (1-x gram) were added in distilled water. To the above solution, 100 ml of ethanol and acetic acid (3:1)V% solution was added and the resultant mixture was vigorously stirred at room temperature for two hours. Another solution was prepared by dissolving 1 g of PVA in 80 ml of distilled water, followed by stirring for 30 minutes at 70°C. The earlier prepared 0.04 M $Zn_{1-x}Co_xO$ solution was drop wise added into PVA solution under continuous stirring for two hours at ambient temperature. The obtained solution was heated at 140°C - 170°C temperature until black powder was obtained. Further, annealing of the black powder was carried out at 700°C in the muffle furnace for two hours. The complete synthesis procedure is schematically shown in the Fig. 1.

3. Results and discussion

To confirm the substitution of Co on Zn sites, the Fourier transform infrared spectra of Co doped samples has been recorded in the 2500-500 cm-1. The position and wavenumber of characteristic peaks in FTIR spectra are not depend merely on crystal structure and chemical composition but also on particle morphology [34]. FT-IR of Co-doped ZnO nanorods at different concentrations of Co^{2+}, is shown in Fig. 2, here ZC002, ZC004, ZC006 and ZC008 represents $Zn_{1-x}Co_xO$ nanorods with x = 0.002, 0.004, 0.006 and 0.008, respectively. The absorption peaks at 501.67 cm^{-1}, 807.45 cm^{-1} and 880.34 cm^{-1} correspond to the telescopic vibration absorption of the Zn–O bond. The peaks at 1096.12 cm^{-1} and 1018.56 cm^{-1} are the telescopic vibrational spectral band of hydroxyl (–OH) group that may be due to the water in the atmosphere and the peak at 1621.49 cm^{-1} corresponds to the absorption of the $>C=O_{str}$ frequency.

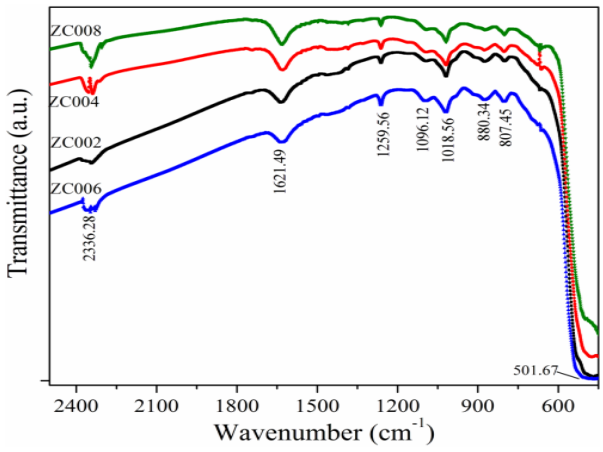

Fig. 2. Fourier Transform Infrared Spectroscopy (FT-IR) of Co-doped ZnO nanorods

The phase purity and crystal structure of the Co-doped ZnO samples were studied by X-ray diffraction (XRD). XRD spectra i.e. Fig. 3 clearly states that the obtained samples are single-phase with wurzite structure whose lattice parameters 'a' and 'c' are independent of Co doping. Similar XRD results of Cobalt doped ZnO have been reported (beyond 1%) [13]. In Fig. 3, ZC002, ZC004, ZC006 and ZC008 represents $Zn_{1-x}Co_xO$ nanorods with x = 0.002, 0.004, 0.006 and 0.008, respectively. From the XRD peaks, the structure of $Zn_{1-x}Co_xO$ was found to be highly crystalline with hexagonal wurzite structure (JCPDS no. 36-1451) [27]. A definite line broadening of the diffraction peaks indicates that the synthesized materials are in nanometer range. In all XRD patterns, the (101) peak is dominant, and its intensity is higher than that of the other peaks, which indicates the preferential growth of [101] orientation along c-axis for all samples. Further, the XRD pattern of the $Zn_{1-x}Co_xO$ shows, the characteristic peaks corresponding to planes (100), (002), (101) have high intensities and peaks (102), (110), (103), (112) have low intensities, that confirms the formation of hexagonal wurzite structure of ZnO. No extra peaks related to cobalt metal, other metal oxides or any zinc-cobalt phase is detected; which clearly indicates that the cobalt dopant appears to reside in the ZnO lattice without precipitation. The obtained samples are of single-phase and the wurzite structures are not influenced by incorporation of Co.

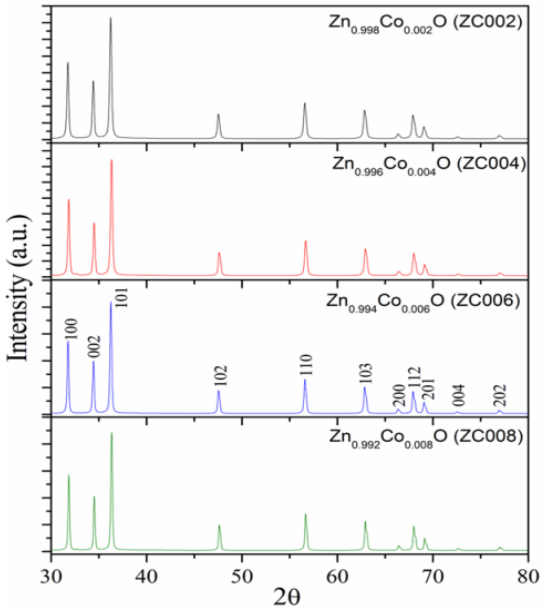

Fig. 3. X-ray diffraction pattern for ($Zn_{1-x}Co_xO$), at x = 0.002, 0.004, 0.006 and 0.008. The nanorods are predominantly c-axis oriented ZnO

The morphology and size of $Zn_{1-x}Co_xO$ (ZC) (x=0.002, 0.004, 0.006 and x=0.008) nanostructures were investigated using a transmission electron microscope (TEM), which confirmed that the obtained structures were nanorods. The micrographs are shown in Fig. 4, confirms the formation of nanorods, with the length ranging from 22-28 nm and diameter 6-9 nm. It can also be noticed from these images that the size of nanorod increases with increasing the doping concentration of cobalt in ZnO.

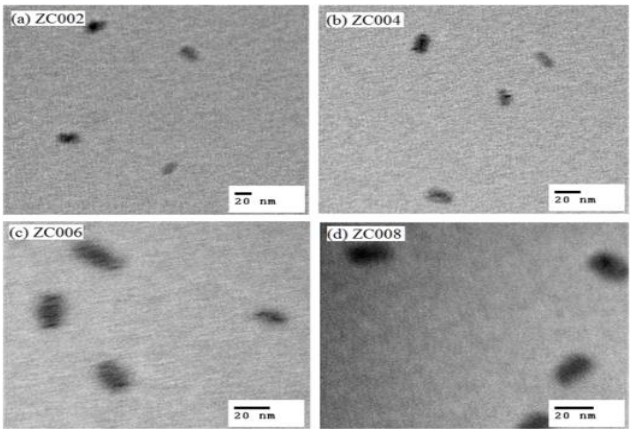

Fig. 4. TEM images of Cobalt doped Zinc nanorods (a) Co doping level 0.2% (b) Co doping level 0.4% (c) Cobalt doping level 0.6% and (d) Co doping level 0.8%

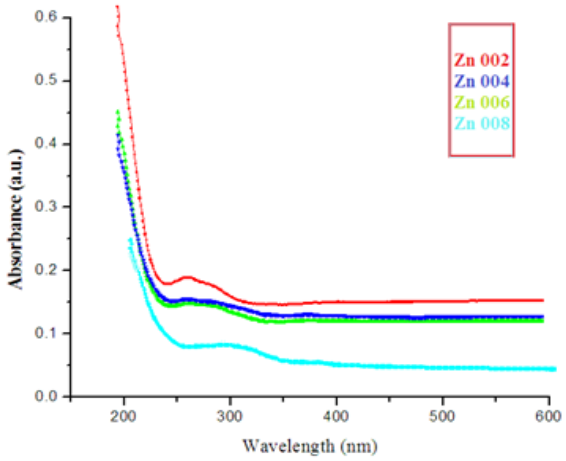

Fig. 5. UV –Vis absorbance of Co-doped ZnOnanorods

The optical properties were explored with UV–Visible, optical absorption study of the samples in the wavelength range of 200-600 nm was recorded are shown in Fig. 5; ZC002, ZC004, ZC006 and ZC008 represents $Zn_{1-x}Co_xO$ nanorods with doping contents x = 0.002, 0.004, 0.006, and 0.008, respectively. The sharp edge of peaks represents samples are with high crystal quality. It is clear from the Fig. 5 that, with the increase in doping concentration from 0.2% to 0.8%, there is shift in the absorbance peaks towards the higher wavelength, which indicates formation of shallow levels inside the band gap by doping. The absorption edges of $Zn_{1-x}Co_xO$ are at 242.54, 246, 247.3 and 249.50 nm for x = 0.002, 0.004, 0.006 and 0.008 respectively. *But it has been reported that, above 1 % doping of Co^{2+}, as one increases the doping concentration there is blue shift in absorbance peaks which signifies broadening of the band gap [32].* The red shift in the band gap E_g edges can be attributed to sp-d exchange interaction between the localized d electrons and band electrons of Co^{2+} substituting the Zn^{2+} ions from crystal lattice [31], [32]. The narrowing of band gap can be interpreted as a result of s-d and p-d exchange interactions, which are leadinjg to positive and negative correction to valance and conduction band edges [33].

Furthermore, the intensity of absorption band is decreasing with the increase in the doping concentration of Co^{2+}; which demonstrates the greater solubility of cobalt at 0.2% and the solubility represents a linear downturn from 0.4% to 0.8%. Similar results have been observed in case of $Zn_{1-x}Co_xO$ nano flask with x ranging from 0.03-0.1 [27].

The magnetic properties of these nanorods were investigated by Vibrating Sample Magnetometer (VSM). The magnetic properties depend on doping concentration of magnetic ions [34]. Paramagnetic behaviour has been reported in ZnO doped with 10% cobalt but with the increase of doping level from 10% to 20% ferromagnetic behavior is observed. Furthermore, the saturation magnetization increased with the increase in the cobalt doping concentration [32]. Fig. 6 represents magnetization (M) versus magnetic field (H) for $Zn_{1-x}Co_xO$ at x = 0.002; 0.004; 0.006; 0.008, which displays asymmetric hysteresis curves. $Zn_{0.998}Co_{0.002}O$and $Zn_{0.994}Co_{0.006}O$ shows ferromagnetism with a clear hysteretic shape. $Zn_{0.996}Co_{0.004}O$ shows mixture of ferromagnetism and antiferromagnetism and $Zn_{0.992}Co_{0.008}O$ shows pure antiferromagnetismand hysteresis shape is irregular. Asymmetry is a function of Co concentration when doping is below 1%.

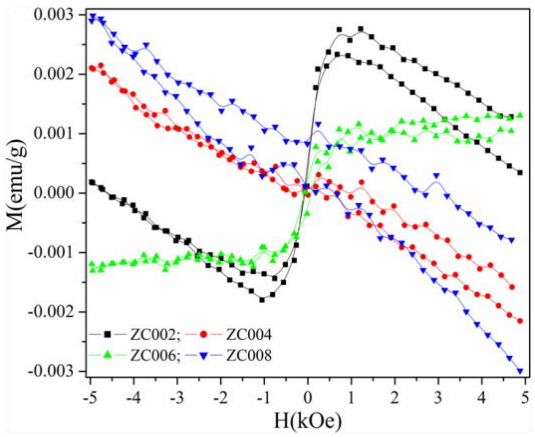

Fig. 6. The graphs of magnetization (M) versus magnetic field (H) for Co doped ZnO nanorods with variation in Co concentration in $Zn_{1-x}Co_xO$ for x = 0.002;0.004; 0.006; 0.008

4. Conclusions

Co-doped ZnO nanorods have been successfully synthesized using sol gel method, with various concentrations of cobalt and the effect of low doping concentration on magnetic and optical properties of $Zn_{1-x}Co_xO$ nonorods have been investigated. UV–Vis optical absorption spectroscopy confirms that, the increase in the doping percentage from 0.2% to 0.8% induces a red shift in the optical band gap of Co-doped ZnO. The observed results are contrary to doping concentration of Co^{2+} above 1% where, the increase in doping concentration results in blue shift. Magnetic hysteresis curves also display irregular behavior at doping less than 1%. The magnetic behavior of $Zn_{1-x}Co_xO$ nanorods changes from ferromagnetic to antiferromagnetic on altering the doping concentrations from 0.2% to 0.8%. The observation made in this study clearly demonstrate that dilute magnetic semiconductor materials can show different magnetic behavior at magnetic ion concentration < 1% than those with magnetic ion concentration above 1%. Thus, doping concentration of Co^{2+} can be used to tune the bandgap and magnetic properties of the ZnO nanorods.

References

[1] S. A. Wolf, Science **294**, 1488 (2001).
[2] I. Žutić, J. Fabian, S. Das Sarma, Rev. Mod. Phys. **76**(2), 323 (2004).
[3] A. Zukova, A. Teiserskis, V. Kazlauskiene, Y. K. Gun'ko, S. van Dijken, J. Magn. Magn. Mater. **316**(2), e203 (2007).
[4] Z. W. Jin, M. Murakami, T. Fukumura, Y. Matsumoto, A. Ohtomo, M. Kawasaki, H. Koinuma, J. Cryst. Growth **214**, 55 (2000).
[5] J. H. Park, M. G. Kim, H. M. Jang, S. Ryu, Y. M. Kim, Appl. Phys. Lett. **84**(8), 1338 (2004).
[6] K. R. Kittilstved, D. A. Schwartz, A. C. Tuan, S. M. Heald, S. A. Chambers, D. R. Gamelin, Phys. Rev. Lett. **97**(3), 2 (2006).
[7] A. C. Tuan, J. D. Bryan, A. B. Pakhomov, V. Shutthanandan, S. Thevuthasan, D. E. McCready, D. Gaspar, M. H. Engelhard, J. W. Rogers, K. Krishnan, D. R. Gamelin, S. A. Chambers, Phys. Rev. B **70**(5), 054424 (2004).
[8] H.-J. Lee, S.-Y. Jeong, C. R. Cho, C. H. Park, Appl. Phys. Lett. **81**, 4020 (2002).
[9] M. Gacic, G. Jakob, C. Herbort, H. Adrian, T. Tietze, S. Brück, E. Goering, Phys. Rev. B **75**(20), 1 (2007).
[10] S. S. Lee, G. Kim, S. C. Wi, J. S. Kang, S. W. Han, Y. K. Lee, K. S. An, S. J. Kwon, M. H. Jung, H. J. Shin, J. Appl. Phys. **99**(8), 08M103 (2006).
[11] A. Barla, G. Schmerber, E. Beaurepaire, A. Dinia, H. Bieber, S. Colis, F. Scheurer, J.-P. Kappler, P. Imperia, F. Nolting, F. Wilhelm, A. Rogalev, D. Müller, J. J. Grob, Phys. Rev. B **76**(12), 125201 (2007).
[12] I. Ozerov, F. Chabre, W. Marine, Mater. Sci. Eng. C **25**(5–8), 614 (2005).
[13] R. Elilarassi, G. Chandrasekaran, Mater. Sci. Semicond. Process. **14**(2), 179 (2011).
[14] E. W. Seelig, B. Tang, A. Yamilov, H. Cao, R. P. H. Chang, Mater. Chem. Phys. **80**(1), 257 (2003).
[15] L. Mädler, W. J. Stark, S. E. Pratsinis, J. Appl. Phys. **92**(11), 6537 (2002).
[16] P. K. Sharma, R. K. Dutta, A. C. Pandey, J. Colloid Interface Sci. **345**(2), 149 (2010).
[17] H. Yang, S. Nie, Mater. Chem. Phys. **114**(1), 279 (2009).
[18] M. Subramanian, M. Tanemura, T. Hihara, V. Ganesan, T. Soga, T. Jimbo, Chem. Phys. Lett. **487**(1–3), 97 (2010).
[19] D. H. Fan, W. Z. Shen, M. J. Zheng, Y. F. Zhu, J. J. Lu, J. Phys. Chem. C **111**(26), 9116 (2007).
[20] J. Elias, R. Tena-Zaera, G. Y. Wang, C. Lévy-Clément, Chem. Mater. **20**(21), 6633 (2008).
[21] K.-K. Kim, N. Koguchi, Y.-W. Ok, T.-Y. Seong, S.-J. Park, Appl. Phys. Lett. **84**(19), 3810 (2004).
[22] T. Busgen, M. Hilgendorff, S. Irsen, F. Wilhelm, A. Rogalev, D. Goll, M. Giersig, J. Phys. Chem. C **112**(7), 2412 (2008).
[23] X. Xu, C. Cao, J. Alloys Compd. **501**(2), 265 (2010).
[24] A. Singhal, S. N. Achary, J. Manjanna, S. Chatterjee, P. Ayyub, A. K. Tyagi, J. Phys. Chem. C **114**, 3422 (2010).
[25] A. Fouchet, W. Prellier, L. Méchin, Superlattices Microstruct. **42**(1–6), 185 (2007).
[26] N. Bahadur, A. K. Srivastava, S. Kumar, M. Deepa, B. Nag, Thin Solid Films **518**(18), 5257 (2010).
[27] F. A. Sigoli, M. R. Davolos, M. Jafelicci, J. Alloys Compd. **262–263**, 292 (1997).
[28] S. Hayashi, N. Nakamori, H. Kanamori, Journal of the Physical Society of Japan **46**(1), 176 (1979).
[29] S. Benramache, B. Benhaoua, H. Bentrah, Journal of Nanostructure in Chemistry **3**, 1 (2013).
[30] H. S. Hsu, J. C. A. Huang, Y. H. Huang, Y. F. Liao, M. Z. Lin, C. H. Lee, J. F. Lee, S. F. Chen, L. Y. Lai, C. P. Liu, Appl. Phys. Lett. **88**(24), (2006).
[31] M. Bouloudenine, N. Viart, S. Colis, A. Dinia, Chem. Phys. Lett. **397(**1–3), 73 (2004).
[32] K. J. Kim, Y. R. Park, Appl. Phys. Lett. **81**(8), 1420 (2002).
[33] P. Koidl, Phys. Rev. B **15**(5), 2493 (1977).
[34] J. M. D. Coey, M. Venkatesan, C. B. Fitzgerald, Nat. Mater. **4**(2), 173 (2005).

*Corresponding author: jaswantece646@gmail.com